Evolving model-free scattering matrix via evolutionary algorithm: ^{16}O-^{16}O elastic scattering at 350 MeV

V. Yu. Korda,[1,*] A. S. Molev,[1,†] and L. P. Korda[1,2]
[1]*Institute of Electrophysics and Radiation Technologies, National Academy of Sciences of Ukraine, 28 Chernyshevsky St., P.O. Box 8812, UA-61002 Kharkov, Ukraine*
[2]*NSC Kharkov Institute of Physics and Technology, National Academy of Sciences of Ukraine, 1 Akademicheskaya St., UA-61108 Kharkov, Ukraine*
(Received 18 April 2005; published 28 July 2005)

We present a new procedure that enables us to extract a scattering matrix $S(l)$ as a complex function of angular momentum directly from the scattering data without any *a priori* model assumptions implied. The key ingredient of the procedure is the evolutionary algorithm with diffused mutation that evolves the population of the scattering matrices by means of their smooth deformations from the primary arbitrary analytical $S(l)$ shapes to the final ones, giving high-quality fits to the data. Because of the automatic monitoring of the scattering-matrix derivatives, the final $S(l)$ shapes are monotonic and do not have any distortions. For the ^{16}O-^{16}O elastic-scattering data at 350 MeV, we show the independence of the final results of the primary $S(l)$ shapes. Contrary to other approaches, our procedure provides an excellent fit by the $S(l)$ shapes that support the "rainbow" interpretation of the data under analysis.

DOI: 10.1103/PhysRevC.72.014611 PACS number(s): 24.10.Ht, 25.70.Bc

I. INTRODUCTION

The S operator is a fundamental quantity of the scattering theory, which incorporates, by a general assumption, all possible information on any possible scattering process (including particle creation or destruction). In the case of elastic scattering, the diagonal matrix elements of the S operator in the angular momentum representation can be given in general form as

$$S(l) = \eta(l)\, e^{2i\varphi(l)}, \tag{1}$$

where the S-matrix modulus $\eta(l)$ and the scattering phase $\varphi(l)$ are real, smooth functions of l. The unitarity of the S matrix for the composite particle–nucleus scattering in the presence of nuclear absorption requires that $\eta(l) \leqslant 1$, so we put

$$\eta(l) = e^{-2\delta_a(l)}, \tag{2}$$

where the nuclear absorption phase $\delta_a(l)$ must be a real, smooth, positive function of l.

Because the colliding nuclei have electric charges, then the scattering phase $\varphi(l)$ can be divided into two parts,

$$\varphi(l) = \delta_r(l) + \sigma_C(l), \tag{3}$$

where the nuclear refraction phase $\delta_r(l)$ and the Coulomb scattering phase $\sigma_C(l)$ must be real, smooth functions of l.

From a general physics viewpoint, the only restrictions we may impose on the nuclear phases $\delta_{a,r}(l)$ to be determined are their finite values at small l, total vanishing at sufficiently large l, and smooth behavior in the intermediate region. The most natural and simple approximation for $\delta_a(l)$ [or $\eta(l)$] and $\delta_r(l)$ is a monotonically descending [for $\eta(l)$, ascending to unity] function that can be easily modeled with the help of, say, Fermi-step or Gauss functions. For the case of elastic heavy-ion scattering at intermediate energies ($\gtrsim$20 MeV/nucleon), the S matrix approaches of such a kind (see, e.g., Refs. [1–4]) and the optical potential models that yield $S(l)$ with such a behavior (see, e.g., Refs. [5,6]) have appeared to be quite successful and argued for the so-called "rainbow" interpretation of the data. However, these models have not allowed an adequate description of all the features of the data measured.

At the same time, in many cases the quality of fit can be improved when the phases $\delta_r(l)$ are modified by additional surface terms of different forms (see, e.g., Refs. [7,8]). Such modifications, in general, make the $S(l)$ dependence nonmonotonic. Note also the S-matrix model with the additional derivativelike interior term in the absorption phase $\delta_a(l)$ [9]. The nonmonotonic behavior of the described type is also inherent in the scattering matrices found with the help of optical potentials that have both the standard Saxon-Woods forms and the ones with the additional surface terms (see, e.g., Refs. [6,10,11]). In spite of the nonmonotonicity of $S(l)$ in these approaches, the rainbow interpretation of the data is, nevertheless, preserved.

Further substantial improvement in the quality of fit is achieved with the help of more flexible $S(l)$ forms that allow the phases to behave nonmonotonically for all relevant l. Such a nonmonotonic behavior is provided by extension of the standard (monotonic) S matrices with a series of the polelike terms (see, e.g., Ref. [12]) or the proper (say, spline) basis functions (see, e.g., Refs. [13–15]). Similar behavior is inherent in the S matrices calculated from the optical potentials that have the additional derivativelike interior terms or have the more complicated forms obtained by use of the spline functions or the Fourier-Bessel series (see, e.g., Refs. [5,16–18]). In spite of the excellence of the quality of fit provided in such approaches, the rainbow interpretation of the data appears to be no longer valid, which raises the

*Electronic address: kvyu@kipt.kharkov.ua
†Electronic address: mas@kipt.kharkov.ua

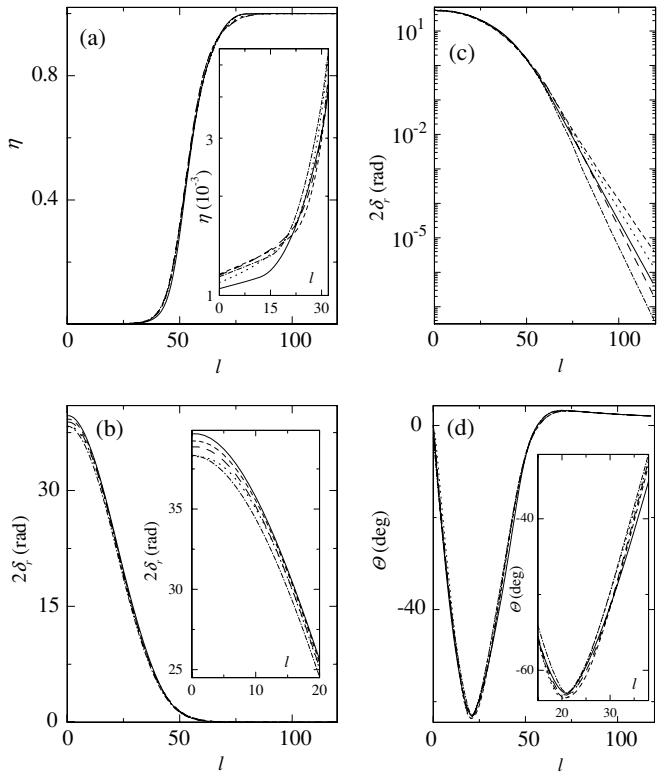

FIG. 1. Five scattering matrices for ^{16}O-^{16}O elastic scattering at 350 MeV, calculated by our procedure with the primary model a for $S(l)$ [Eq. (4)]: (a) Scattering-matrix moduli $\eta(l)$. The inset shows the region of small momenta in the logarithmic scale. (b) Nuclear phases $\delta_r(l)$. The inset shows the region of small momenta in the enlarged scale. (c) The same as (b) but in logarithmic scale. (d) Deflection functions $\Theta(l)$. The inset shows the vicinity of $\Theta(l)$ minima in the enlarged scale. Solid curves correspond to the best quality of fit to the data $\chi^2 = 2.4$.

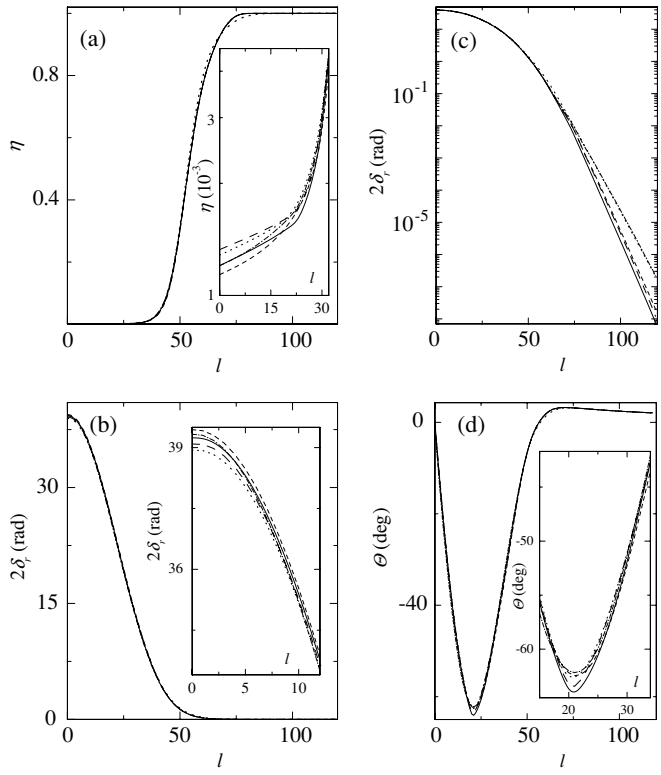

FIG. 2. The same as Fig. 1 but with primary model b for $S(l)$ [Eq. (5)].

problem of finding the physical meaning of the results obtained this way.

Clearly all the approaches just mentioned are more or less model dependent because the functions used to model the phases $\delta_{a,r}(l)$ and the real and imaginary parts of optical potential $V(r)$ and $W(r)$ are more or less the properly parametrized analytical ones. Thus the search spaces of all possible shapes for the S matrix and the optical potential are strongly reduced, and consequently data analyses performed on such spaces can lead to an incorrect physical interpretation of the data.

That is why it would be highly desirable to have a procedure that could extract the scattering matrix and/or the optical potential directly from the experimental data without the introduction of any bias toward some *a priori* "physically reasonable" model assumptions. The very first question this procedure must answer is whether the nonmonotonic (or polelike) structures and any other distortions that appear in the S-matrix shapes obtained in the most successful approaches are really necessary for reproducing the experimental data studied. This will help us to shed more light on the applicability of the rainbow interpretation to the heavy-ion collisions in the wide range of energies and mass numbers.

II. MODEL-FREE DETERMINATION OF THE SCATTERING MATRIX

To develope the desired procedure that determines $S(l)$ directly from the data, data $\longrightarrow S(l)$, we need to solve the problem in its most explicit form, in which each value of $\delta_{a,r}(l)$ is treated generally as an independent fitting parameter. This makes the problem parameter space highly dimensional and the choice of an appropriate search method crucial. Evolutionary (or genetic) algorithms (EAs) have many times proved very efficient in dealing with very difficult physical problems (see, e.g., Refs. [19–22]), so we have chosen an EA as a key element of our procedure. Note that our algorithm resembles the so-called smooth genetic algorithm proposed in Ref. [23].

According to the general ideology of the EA implementation, we deal with the population of N individuals. Each individual is the S matrix presented as a pair of real-valued $l_{\max}$-dimensional vectors $[\delta_a(l), \delta_r(l)]$, $l = 0, 1, \ldots, l_{\max} - 1$. The fitness of each individual reflects the quality of data fitting provided by the individual's S matrix. By using the mutation operation the algorithm evolves the initial population of the badly fitted individuals to the final population of the highly fitted ones.

Every iteration of our procedure contains the following steps.

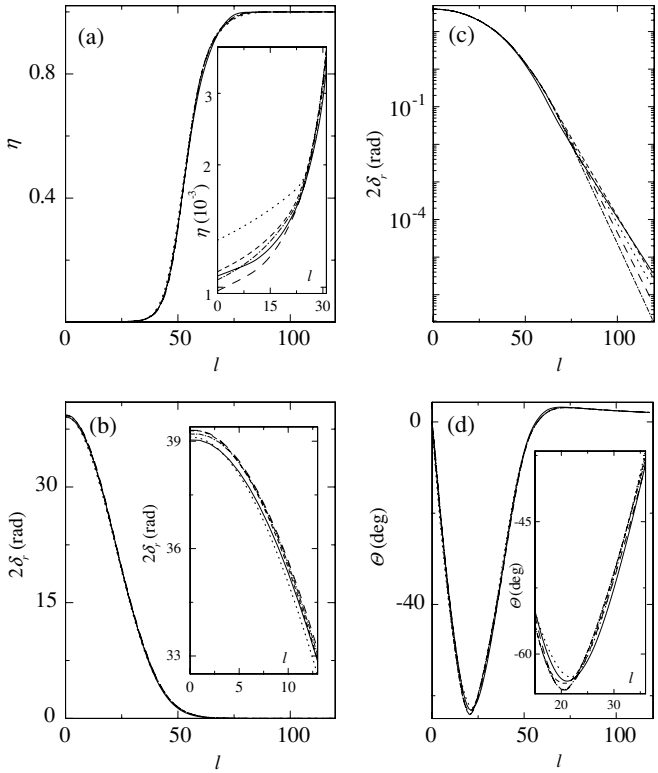

FIG. 3. The same as Fig. 1 but with primary model c for $S(l)$ [Eq. (6)].

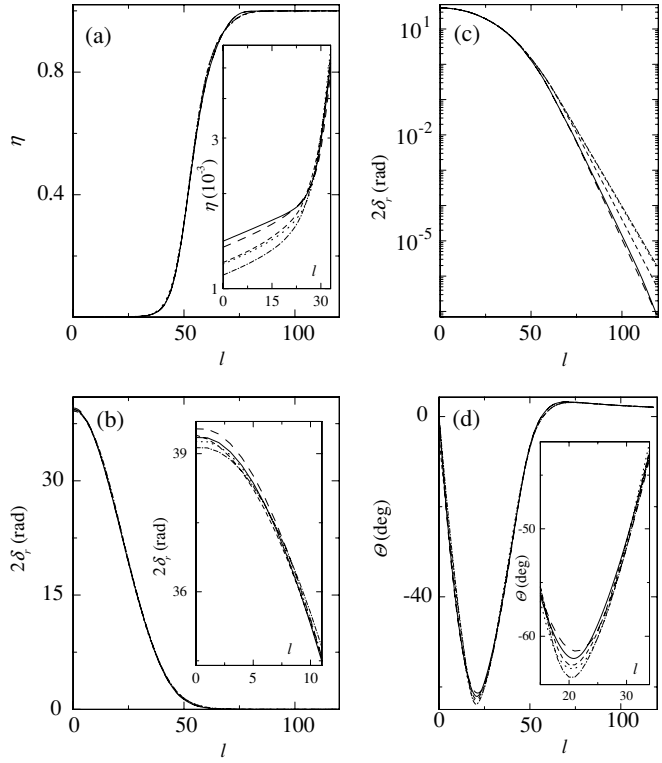

FIG. 4. The same as Fig. 1 but with primary model d for $S(l)$ [Eqs. (7)].

(1) Generating the initial population of N individuals. For each individual, the vectors $\delta_{a,r}(l)$ are filled with the help of any monotonically descending function of l, the first derivative of which has only one minimum. To be definite and to test the robustness of the procedure against various starting conditions, we choose the following five primary models for $S(l)$.

a. The six-parameter model composed of two Fermi functions:

$$2\delta_i(l) = g_i\, f(l, l_i, d_i),$$
$$f(l, l_i, d_i) = \left[1 + \exp\left(\frac{l - l_i}{d_i}\right)\right]^{-1},$$
$$i = a, r. \tag{4}$$

b. The four-parameter model composed of two Gaussian functions:

$$2\delta_i(l) = g_i \exp\left(-\frac{l^2}{d_i^2}\right). \tag{5}$$

c. The five-parameter McIntyre model [1]:

$$\eta(l) = f(-l, -l_a, d_a),$$
$$2\delta_r(l) = g_r\ \ f(l, l_r, d_r). \tag{6}$$

d. The six-parameter phenomenological model [4]:

$$2\delta_i(l) = g_i\Big[(2l+1)\, d_i F(l, l_i, d_i) + d_i^2 F^2(l, l_i, d_i)\Big]^{1/2} f^{p_i}(l, l_i, d_i),$$
$$F(l, l_i, d_i) = -f^{-1}(l, l_i, d_i)\ln\left[1 - f(l, l_i, d_i)\right],$$
$$p_a = 1, \quad p_r = 2. \tag{7}$$

e. The six-parameter model composed of two power-type functions:

$$2\delta_i(l) = \frac{g_i}{l^{\alpha_i} + \beta_i}, \quad \alpha_i > 2. \tag{8}$$

The parameters g_i, l_i, d_i, α_i, and β_i are positive. They are chosen for each individual and each model function at random within some intervals that are wide enough to produce substantially different shapes of the phases. Normally, all the individuals in a given population are initialized with one and the same function from the set a–e.

All the mentioned primary models for $S(l)$ are "physically justified," except for case e, which has no physical background. Nevertheless, we have included this purely mathematical case to see whether the procedure is able to find "physically meaningful" results under such a tough conditions.

(2) Evaluating the fitness of each individual in the population. The fitness function in our approach consists of two parts. The first one is associated with the quality of the shapes of $\delta_{a,r}(l)$, and the second one accounts for the quality of the fitting of the experimental data.

The requirements that the shapes of $\delta_{a,r}(l)$ must meet in our approach are as follows:

i. The functions $\delta_{a,r}(l)$ must be descending.

ii. The first derivatives of $\delta_{a,r}(l)$ must have only one minimum and no maxima.

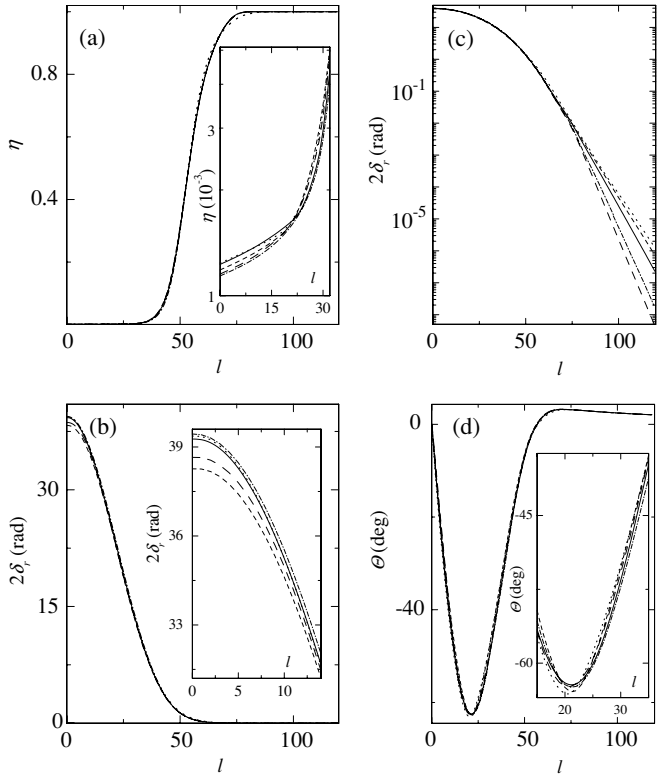

FIG. 5. The same as Fig. 1 but with primary model e for $S(l)$ [Eq. (8)].

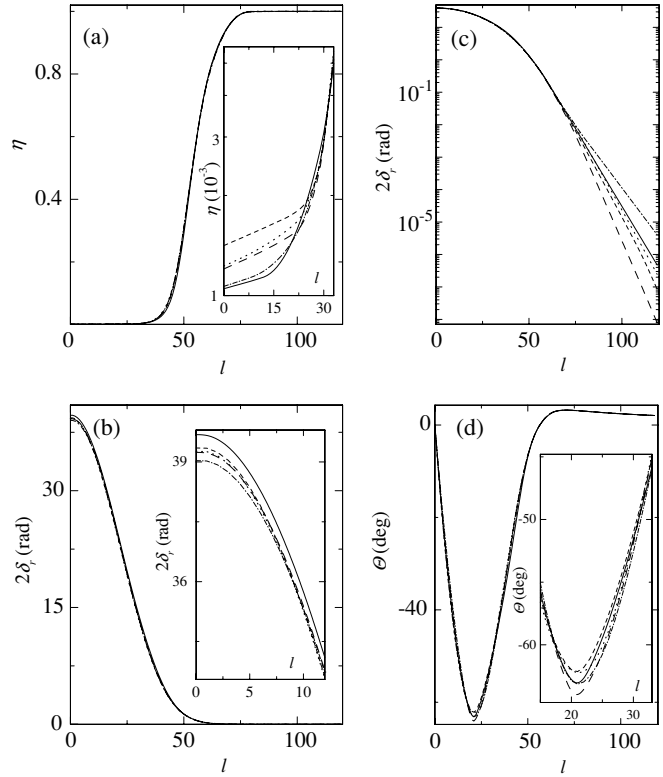

FIG. 6. Five best results from Figs. 1–5. Notation is the same as in Fig. 1.

iii. The second derivatives of $\delta_{a,r}(l)$ must not have more than one minimum and one maximum.

iv. The third derivative of $\delta_r(l)$ must not have more than one minimum and one maximum.

v. The logarithmic derivative of $\delta_r(l)$ must be descending.

Requirements i–iii ensure the absence of any distortions of the phase shapes, at least up to the second-order derivatives. Condition iv is added because we want the deflection function $\Theta(l) \equiv 2d\varphi(l)/dl$ to have no shape distortions up to the same order of its derivatives. Condition v provides for the permanent decrease of $\delta_r(l)$ with the increase of l. Requirements i–iv are crucial for the shapes of $\delta_{a,r}(l)$. Thus the penalties imposed on the individual in the case of violation of these requirements are fatal. Condition v is not so strong and introduces only the ultimate bias toward the desired tail of $\delta_r(l)$.

The quality of the fit of the calculated differential cross section to the experimentally measured one is assessed by means of the standard χ^2 magnitude per data point. The calculations are made by use of the expansion of the scattering amplitude into a series of Legendre polynomials. The elastic-scattering differential cross section is equal to the squared modulus of this amplitude.

It is often claimed that the amount of the large scattering angle data is insufficient to determine the scattering matrix and/or the optical potential in a unique way. Thus we add several additional pseudo data points after the last actual ones, which follow the tendency of the cross-section behavior (see, e.g., Ref. [14]). Of course, this prescription cannot be universal and must be used with care in the context of the data under study. The incorporation of the invented data points to the χ^2 criterion can appear misleading for the fitting procedure; therefore we use the penalty-free corridor around those points and apply the prescription only after the fitting to the actual data set has been accomplished.

(3) Letting each individual in the population produce M offspring. The replication is performed according to the transformation:

$$\log[\delta_i'(l)] = \log[\delta_i(l)] + A_i\, N_i(0,1)\, D(l, l_{m,i}, d_{m,i}), \qquad i = a, r, \tag{9}$$

where $\delta_i(l)$ and $\delta_i'(l)$ are the parent's and the offspring's S-matrix phases, respectively, $A_i > 0$ is the mutation amplitude, $N_i(0,1)$ denotes a normally distributed one-dimensional random number with mean zero and one standard deviation, $l_{m,i}$ stands for the mutation point chosen randomly in the interval $0 \leqslant l_{m,i} \leqslant l_{\max} - 1$, and $d_{m,i} > 0$ is the value characterizing the diffuseness of the mutation point. The diffusing function $D\left(l,\ l_{m,i},\ d_{m,i}\right)$ must be of a bell-like shape with the only maximum at $l = l_{m,i}$ and the falloff tail around this point. To be definite and to ensure the proper localization of the consequences of the mutation, we choose the diffusing function in the

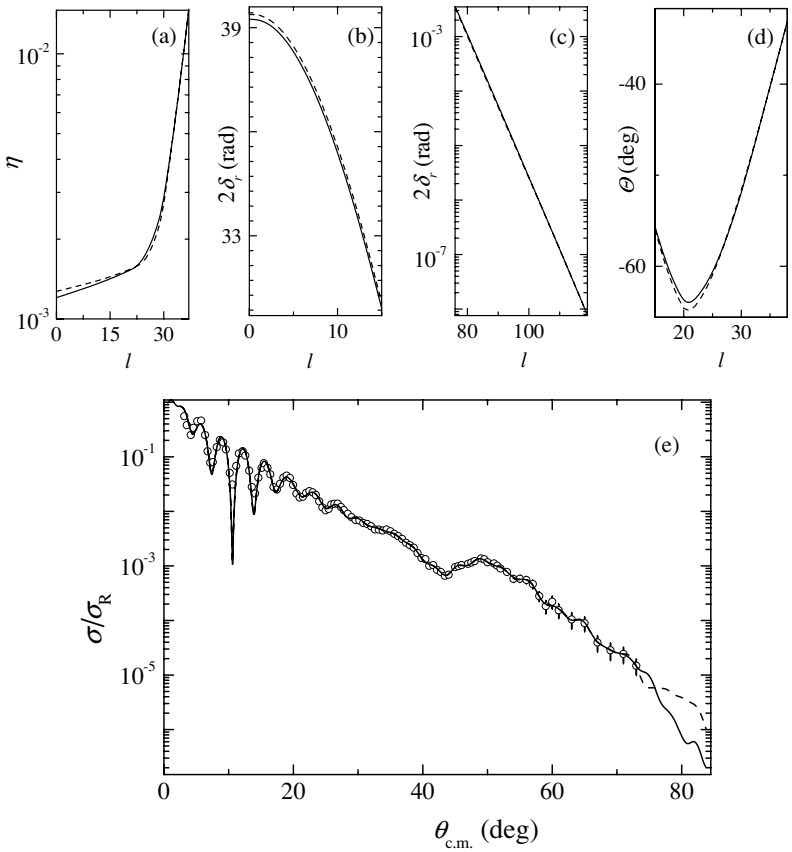

FIG. 7. Two scattering matrices and differential cross sections for ^{16}O-^{16}O elastic scattering at 350 MeV, calculated by our procedure with primary model b for $S(l)$ [Eq. (5)]. Solid (dashed) curves are the results of calculations with the invented data points taken (not taken) into account in the region of large scattering angles. (a) Scattering matrix moduli $\eta(l)$ and (b) nuclear phases $\delta_r(l)$ in the region of small momenta; (c) $\delta_r(l)$ in the region of large momenta; (d) deflection functions $\Theta(l)$ in the vicinity of the minima; (e) the differential cross sections (ratio to Rutherford). Experimental data are taken from Refs. [25] and [26]. Solid curves presenting $S(l)$ correspond to the same ones shown in Fig. 2.

following form:

$$D(l,\ l_{m,i},\ d_{m,i}) = \exp\left[-\frac{(l-l_{m,i})^2}{d_{m,i}^2}\right]. \qquad (10)$$

The mutation amplitude A_i and the mutation diffuseness $d_{m,i}$ are the quantities automatically tuned within some intervals. The limits of these intervals, having extremely large values at the beginning of the procedure, are smoothly decreased in the course of the run and acquire small values at the end. Such a schedule provides for both the removal of the features of the primary parametrizations a–e from the individual's $S(l)$ and the fine tuning of the details of $S(l)$.

(4) Evaluating the fitness values of all offspring. Sort the offspring in descending order according to their fitnesses. Select N best offspring to form the new population.

(5) Going to step 3 or stopping if the best fitness in the population is sufficiently high (the χ^2 value is small enough).

EAs make up, generally, the global optimization technique that, however, cannot guarantee that the optimum found is the global one. Therefore it is necessary to run the procedure several times. Besides, there is no way to know in advance what the minimum value of the χ^2 magnitude will be. Thus it is instructive to monitor the dynamics of the best, worst, and mean fitness values and the rms deviation from the mean fitness in the population during those several runs of the procedure. Such monitoring usually helps to localize the region of the potentially lowest χ^2 values.

III. SCATTERING MATRIX FOR ^{16}O-^{16}O ELASTIC SCATTERING AT 350 MeV

We applied our technique to analyze the well-known test case of ^{16}O-^{16}O elastic scattering at 350 MeV, for which the approaches that give a very good quality of fit predict the existence of the nonmonotonic structures in the S matrix (see, e.g., Refs. [12,13]).

In our calculations, bearing in mind that the collision energy is sufficiently high, we let $\sigma_C(l)$ in Eq. (3) be the quasi-classical phase of the point-charge scattering by the uniformly charged sphere (see, e.g., Ref. [3]) having the radius $R_C = 0.95 \times 2 \times 16^{1/3}$ [24]. The calculated differential cross sections were symmetrized for the scattering of identical nuclei. The experimental errors are assumed to be equally weighted (10% error bars).

Figures 1–5 show the results of our calculations with primary models a–e for $S(l)$, respectively. The χ^2 values for our fits to the data are 2.4−2.5. For each initial case, the results of five different runs of the procedure are presented to display the error bands within each of the primary $S(l)$ models. Figure 6 compiles the five best results from Figs. 1–5 to illuminate their sensitivity to the details of the particular primary $S(l)$ model. Figure 7 demonstrates the consequences of consideration of the invented data points in the region of large scattering angles.

IV. DISCUSSION

The evolutionary procedure of determining the scattering matrix presented in this article is aimed at searching for the globally optimal solution. However, being aware of the complexity of the problem under study and the fact that the actual number of fitting parameters (twice the number of angular momenta, which is $l_{\max} = 120$ in our test case) is substantially greater than the actual number of data points (which is equal to 105 in our test case), we do not expect to achieve it. Therefore we consider the obtained results (Figs. 1–7) as very promising.

First, we see that, within every model used for the primary $S(l)$ dependence, regardless of the variety of their shapes, the moduli $\eta(l)$ and the nuclear refraction phases $\delta_r(l)$, as well as the total deflection functions $\Theta(l)$, obtained in different runs of the procedure, go close to each other (Figs. 1–5). The differences among them can sometimes be seen only in the enlarged or even logarithmic scale. The same observation can be made if one analyzes the compilation of the best results (Fig. 6), which points out their independence of the initial conditions. At the same time, the nuclear phases $\delta_r(l)$ deviate from each other in the region of large angular momenta. There the scattering matrix moduli $\eta(l)$ are very close to unity, which makes the contributions of the partial waves with these values of l to the scattering amplitude vanishingly small. To introduce the corresponding bias into the searching procedure, we probably need more precise experimental information in the region of small scattering angles. Nevertheless, we are able to conclude that, under requirements i–v imposed on the phases $\delta_{a,r}(l)$, we have managed to localize the region of the scattering-matrix shapes that gives the lowest values to the χ^2 magnitude.

It is important to emphasize the remarkable fact that the application of power-type function e [Eq. (8)] as the primary $S(l)$ parametrization, which has no proper physical meaning, does not produce any difficulties for our procedure to find the physically meaningful scattering matrix (Fig. 5). From the formally mathematical viewpoint, the iterative application of replication transformation (9) to the phases $\delta_{a,r}(l)$ is equivalent to the addition to the primary phases of the ultimately "infinite" sum of diffusing function (10) with various parameters and weights. Because of the special schedule of choosing and tuning the latter, the phase shapes are transformed almost adiabatically across the run of the procedure. As a result, the phases evolve to equilibrium, with respect to the fitness, shapes that are free from any recollections about the particular models for the primary $S(l)$ and the diffusing function. That is why, we believe, our procedure is actually a model-free one.

It is somewhat surprising that the incorporation of the additional pseudo data points in the fitness function, which really forces the cross section to behave as desired, produces no noticeable corrections to the scattering matrix (Fig. 7) in the whole range of l. This is against the conventional way of thinking, but could be just a feature of that particular data set under study.

From the physics viewpoint, our results support the rainbow interpretation of the given data: The maximum in the differential cross section observed near 50° is identified as the primary nuclear rainbow. The nuclear rainbow angle that corresponds to the minimum of the deflection function $\Theta(l)$ acquires the values $\theta_r = 61^\circ$–64°. At this point, one might ask whether it is possible to improve the quality of fit, bearing in mind the number of fitting parameters. In fact, the answer is positive. If, from the very beginning, we abandon all requirements i–v imposed on the shapes of $\delta_{a,r}(l)$, then the procedure becomes able to find the results with $\chi^2 \approx 0.5$–0.6. However the S matrices for these cases are nonmonotonic and substantially different from run to run, belonging to different local optima. The other way to search for a better quality of fit could be found in testing the stability of the monotonic shapes of the S-matrices obtained in our study against nonmonotonic transformation (9). Then it seems more probable to find the results that belong to the same local optimum or the nearest ones. Following this way, if and only if the substantial improvement in the quality of fit is accompanied by repeated observations of the same equilibrium nonmonotonic structures in $S(l)$, then one should admit that the appearance of these structures is necessary and the search for their physical interpretation urgent.

The proposed recipe can also be useful in analyzing some important cases in which the presence of nonmonotonic (or even nonsmooth) structures in the S matrix seems to be justified; namely, those cases in which, for instance, the behavior of $S(l)$ is resonance dominated (see, e.g., Refs. [6,27]), or it is important to account for the dynamic effects (parity dependence of the interactions between nuclei, elastic transfer; see, e.g., Refs. [28,29]), or the interference effects condition the nonmonotonic scattering matrices (see, e.g., Ref. [10]). To confirm the existence of the discussed equilibrium structures in the S matrix, we need to extract them directly from the respective experimental data, using, for instance, our approach with requirements i–v switched off either from the very beginning or after the monotonic shape of the S matrix is obtained. If we succeed, then we must admit that requirements i–v cannot apply to all cases.

The evolutionary procedure presented in this article has been initially devised to determine the scattering matrix in the angular momentum representation. Obviously, a similar approach can be used to develop the evolutionary procedure for the determination of radial dependence of a complex optical potential. With the help of this procedure, the optical potential can be extracted directly from the experimental data: data $\longrightarrow$ $V(r)$. Moreover, with the similar procedure, the scattering matrix produced by the optical potential can be fitted to the scattering matrix extracted directly from the data: data $\longrightarrow$ $S(l) \longrightarrow V(r)$. This means that the optical potential found in this way will correspond to the scattering matrix extracted immediately from the data. Having unified these three search procedures, data $\longrightarrow S(l)$, data $\longrightarrow V(r)$, and data $\longrightarrow$ $S(l) \longrightarrow V(r)$, into one, we obtain a powerful tool for the deep theoretical investigation of heavy-ion collisions at intermediate energies.

ACKNOWLEDGMENT

This work was supported in part by The State Fund of Fundamental Research of Ukraine, grant no. 02.07/372.

[1] J. A. McIntyre, K. H. Wang, and L. C. Becker, Phys. Rev. **117**, 1337 (1960).
[2] S. K. Kauffmann, Z. Phys. A **282**, 163 (1977).
[3] Yu. A. Berezhnoy and V. V. Pilipenko, Mod. Phys. Lett. A **10**, 2305 (1995).
[4] Yu. A. Berezhnoy and A. S. Molev, Int. J. Mod. Phys. E **12**, 827 (2003).
[5] A. M. Kobos, M. E. Brandan, and G. R. Satchler, Nucl. Phys. **A487**, 457 (1988).
[6] M. E. Brandan and K. W. McVoy, Phys. Rev. C **43**, 1140 (1991).
[7] G. Hauser, R. Löhken, H. Rebel, G. Schatz, G. W. Schweimer, and J. Specht, Nucl. Phys. **A128**, 81 (1969).
[8] Yu. A. Berezhnoy and V. V. Pilipenko, J. Phys. G **11**, 1161 (1985).
[9] A. S. Molev, V. Yu. Korda, and L. P. Korda, Izv. Ross. Acad. Nauk Ser. Fiz. **68**, 205 (2004).
[10] N. Austern, Ann. Phys. (NY) **15**, 299 (1961).
[11] S. N. Ershov, F. A. Gareev, R. S. Kurmanov, E. F. Svinareva, S. G. Kazacha, A. S. Dem'yanova, A. A. Ogloblin, S. A. Goncharov, J. S. Vaagen, and J. M. Bang, Phys. Lett. **B227**, 315 (1989).
[12] L. J. Allen, L. Berge, C. Steward, K. Amos, H. Fiedeldey, H. Leeb, R. Lipperheide, and P. Fröbrich, Phys. Lett. **B298**, 36 (1993).
[13] S. G. Cooper, M. A. McEwan, and R. S. Mackintosh, Phys. Rev. C **45**, 770 (1992).
[14] M. A. McEwan, S. G. Cooper, and R. S. Mackintosh, Nucl. Phys. **A552**, 401 (1993).
[15] S. G. Cooper and R. S. Mackintosh, Nucl. Phys. **A582**, 283 (1995).
[16] M. C. Mermaz, Phys. Rev. C **47**, 2213 (1993).
[17] M. P. Nicoli, F. Haas, R. M. Freeman, S. Szilner, Z. Basrak, A. Morsad, G. R. Satchler, and M. E. Brandan, Phys. Rev. C **61**, 034609 (2000).
[18] M. Ermer, H. Clement, G. Frank, P. Grabmayr, N. Heberle, and G. J. Wagner, Phys. Lett. **B224**, 40 (1989).
[19] J. R. Morris, D. M. Deaven, and K. M. Ho, Phys. Rev. B **53**, 1740(R) (1996).
[20] K. Michaelian, Evolving an energy dependent optical model description of heavy-ion elastic scattering, Rev. Mex. Fis. **42** (suppl. 1), 203 (1996).
[21] C. Winkler and H. M. Hofmann, Phys. Rev. C **55**, 684 (1997).
[22] S. V. Berezovsky, V. Yu. Korda, and V. F. Klepikov, Phys. Rev. B **64**, 064103 (2001).
[23] M. W. Gutowski, J. Phys. A **27**, 7893 (1994).
[24] M. E. Brandan and G. R. Satchler, Nucl. Phys. **A487**, 477 (1988).
[25] E. Stilliaris, H. G. Bohlen, P. Fröbrich, B. Gebauer, D. Kolbert, W. von Oertzen, M. Wilpert, and Th. Wilpert, Phys. Lett. **B223**, 291 (1989).
[26] M. E. Brandan and G. R. Satchler, Phys. Lett. **B256**, 311 (1991).
[27] K. W. McVoy, Phys. Rev. C **3**, 1104 (1971).
[28] W. E. Frahn, Nucl. Phys. **A337**, 324 (1980).
[29] W. E. Frahn, M. S. Hussein, L. F. Canto, and R. Donangelo, Nucl. Phys. **A369**, 166 (1981).